Interpretation of Sum Frequency Generation Vibrational Spectra of Interfacial Proteins by the Thin Film Model

Jie Wang, Zoltan Paszti, Mark A. Even, and Zhan Chen*

Department of Chemistry, University of Michigan, 930 North University Avenue, Ann Arbor, Michigan 48109

Received: October 6, 2003; In Final Form: January 10, 2004

To interpret sum frequency generation (SFG) vibrational spectra collected from adsorbed protein molecules using structures of the interfacial proteins, the thin film model has been evaluated both theoretically and experimentally. The calculations indicate that nonlocal contributions to SFG spectra of interfacial proteins usually can be ignored. The experimental results indicate that for some polarization combinations, such as ssp and sps, local field variations across the adsorbed protein layer will not substantially affect SFG signals. Therefore, SFG spectra collected from adsorbed protein molecules are generally dominated by the electric-dipole contribution. From such spectra, quantitative structural or conformation information about interfacial proteins can be deduced using the thin film model. As an example, we analyzed the orientation distribution of the methyl groups of BSA molecules at different interfaces.

1. Introduction

Protein adsorption is one of the most important processes occurring on solid surfaces immersed into biological fluids. Understanding protein adsorption is a crucial step in developing biomaterials or controlling biofouling. In the past few decades, it has been extensively studied by various experimental techniques. [1−10]

Recently, sum frequency generation (SFG) vibrational spectroscopy has been applied to study protein adsorption.[11−18] SFG is a second-order nonlinear optical process, which can provide information about average orientation and orientation distribution of chemical groups within an optical field. It is surface/interface sensitive under the electric-dipole approximation, which is valid for many systems.[19−38] Research on protein adsorption demonstrates that SFG can selectively detect interfacial proteins with excellent interface specificity. Although qualitative studies of conformation changes of adsorbed protein molecules at different interfaces using SFG have been reported, in depth quantitative analysis of interfacial protein structure/conformation has not been achieved yet.

The interpretation of general SFG measurements is usually based on an infinitesimally thin interface layer model, which considers a thin and well-defined "interface" between two semi-infinite contacting media. For this model, both the molecular structure and optical field inside this interface are considered uniform.[19,39] Such a model is valid to treat most sharp interfaces and adsorption of small molecules on a surface. However, for protein adsorption studies, this model needs to be examined because proteins are large molecules and therefore the infinitesimally thin interface layer model may not be valid. An adsorbed protein layer can be several nanometers thick; thus SFG spectra collected from such a protein layer may be affected by variations of the local optical field. [40]

As a result, SFG studies on protein adsorption cannot necessarily be considered as a natural extension from SFG studies on other materials, e.g., polymers. In the case of a polymer film (which is usually much thicker than a protein monolayer), it is generally believed that the signal is dominated by the electric dipole contribution and arises from the uppermost part, i.e., the polymer/ambient interface, which is supported by several experimental results.[29] The reason for this behavior is that regions just beneath the surface can be regarded to be at least locally centrosymmetric, leading to cancellation of the electric dipole signals. In the case of a protein monolayer, however, at this moment it seems to be very difficult to determine the depth distribution of the SFG active groups. In such a case, we have to sum up the contributions through the thickness of the film, as described in ref 21. The results, as we will show in this work, reflect not only an orientational average of the studied groups over the Euler-angles, as in the case of a polymer surface, but also a spatial average over the film thickness. This is an important conceptual extension of the SFG data analysis.

In addition to the infinitesimally sharp interface model, research has been done to interpret SFG spectra using other models.[14,41] In our previous publications, we adopted a more general thin film model to qualitatively study protein adsorption.[14] We found that the SFG signal from an adsorbed protein layer is sensitive to the change of interfacial environment rather than the change of refractive index of contacting media or the local field variation across the protein layer. This indicates that the dipole (i.e., local) contribution still dominates the SFG spectrum because the nonlocal contribution depends more on the refractive index change across the film.[42] However, more details about this model need to be worked out.

In this paper, the thin film model for protein adsorption has been studied in depth both theoretically and experimentally. Theoretically, we estimated the nonlocal contributions to the SFG signals of a protein layer. We found that under our experimental conditions it is usually much smaller than the dipole contribution and thus can be ignored here. This conclusion provides theoretical support to our former experimental results.[14,15] However, even if the nonlocal contributions are

* To whom all correspondence should be addressed. E-mail: zhanc@umich.edu. Fax: 734-647-4865.

10.1021/jp0370019 CCC: $27.50
Published on Web 02/25/2004

negligible, changes in the local optical field may affect SFG signals. Therefore, using appropriate model systems, we evaluated the effect of variations in the local optical field across a thin film on the measured SFG spectra. From our analysis, we found that under our experimental conditions the SFG spectrum of an adsorbed protein layer is mostly determined by the molecular structure of the interfacial protein molecules. Therefore, it is possible to acquire quantitative orientation and/or conformation information about adsorbed protein molecules by SFG measurement.

The importance of bulk effects in quantitative nonlinear optical experiments has been treated extensively in the literature.[20,43,44] We have to make, however, a distinction between "bulk contributions" due to the slow variation of the electric field inside the bulk of a material and further nonlocal contributions arising from the rapid field variation at interfaces. In this paper, we consider adsorbed protein layers in the nanometer thickness regime (i.e. monolayer protein adsorption), and we expect that only the latter effect may contribute significantly to the measured spectra. We use the term "nonlocal contribution" instead of "bulk contribution" in order to emphasize this distinction, which, at the same time, allows us to neglect phase variation effects inside the film. The local field correction factor and average refractive index have been studied for interface or bulk environments.[45−48] However, evaluation of the local optical field by considering both variations of the local field correction factor and local refractive index across a thin film (several nanometers) is necessary, and it has not been convincingly solved yet. The current treatment often simply ignores the local field correction factor or treats it as a constant for an interfacial layer; this treatment is sufficient for a sharp interface but may not be suitable for a thin protein film. The layout of this paper is the following: first, we estimate the nonlocal contribution by calculation to show that it is reasonable to ignore such contributions for SFG signals collected from interfacial protein molecules in most cases; then we use SFG experiments to demonstrate that, for the dipole contribution, variation of the local field will not affect the ssp or sps SFG signals substantially, showing that the thin film model is valid; thus from SFG spectra we can deduce interfacial structural/conformation information on protein molecules; finally, we use the thin film model to quantitatively deduce the orientation and orientation distribution of methyl groups of interfacial bovine serum albumin (BSA) molecules at different interfaces.

2. Calculation

2.1. Estimation of the Nonlocal Contribution. The basic framework of the thin film model has been applied in optical physics research for decades. It is also used to interpret SFG and second harmonic generation (SHG) experiments.[14,41] Our aim here is to apply this model to quantitative SFG studies on protein adsorption. First, we want to confirm by a reasonable order of magnitude estimation that the electric-dipole approximation is still valid for an adsorbed protein layer on fused silica or polymer surfaces, which were used in our experiments.

We start with the general formulation of the thin film model. Let us imagine a thin nonlinear layer of thickness d in the $x-y$ plane, which is sandwiched between a semi-infinite ambient at $z \geq d$ characterized by a refractive index of n_1 and a semi-infinite substrate at $z \leq 0$ with refractive index n_2. The optical properties of both the substrate and the ambient are strictly linear. The excitation beams are incident in the $x-z$ plane from the substrate side. The second-order nonlinear polarization field $\mathbf{P}^{(2)}(\omega_{SF} = \omega_{VIS} + \omega_{IR},\mathbf{r})$ induced by the two optical fields $\mathbf{E}(\omega_{VIS},\mathbf{r})$ and $\mathbf{E}(\omega_{IR},\mathbf{r})$ is

$$\mathbf{P}^{(2)}(\omega_{SF},\mathbf{r}) = \vec{\vec{\chi}}^{D}(\mathbf{r}):\mathbf{E}(\omega_{VIS},\mathbf{r})\mathbf{E}(\omega_{IR},\mathbf{r}) + \Phi^{D}(\mathbf{r}) + \vec{\vec{\chi}}^{P_1}(\mathbf{r}):\nabla\mathbf{E}(\omega_{VIS},\mathbf{r})\mathbf{E}(\omega_{IR},\mathbf{r}) + \vec{\vec{\chi}}^{P_2}(\mathbf{r}):\mathbf{E}(\omega_{VIS},\mathbf{r})\nabla\mathbf{E}(\omega_{IR},\mathbf{r}) - \nabla\cdot[\vec{\bar{\chi}}^{Q}(\mathbf{r}):\mathbf{E}(\omega_{VIS},\mathbf{r})\mathbf{E}(\omega_{IR},\mathbf{r})] + ... \quad (1)$$

where the first term describes the electric-dipole driven nonlinear response, the second term denotes the contribution $\Phi^{D}(\mathbf{r})$ related to the electrostatic field $\mathbf{E}_0(\mathbf{r})$, which is produced by the charged protein molecules in the adsorbed layer. This electrostatic field may make an additional contribution to the nonlinear polarization by a third-order nonlinear process;[25] however, it is usually very small especially when the net charges on the protein molecules are close to zero and can be ignored in our following considerations.[14] The third, fourth, and fifth terms stand for electric quadrupole driven contributions, which already include the magnetic-dipole contribution.[20,49]

The electric-dipole contribution (the first term in eq 1) depends sensitively on the structure of the material and will not change very much with variation of the optical field, as will be shown in sections 2.2 and 3.2. The electric-quadrupole-type contributions are, however, nonlocal in their character and, as a result, highly sensitive to variation of the optical field. Usually the dipole contribution is used to analyze SFG spectra. However, if contributions from other terms in eq 1 are dominant or comparable in magnitude, such analysis may induce errors.

It is well established that the sum frequency intensity radiated by the induced nonlinear polarization (shown in eq 1) can be related to the product of the input intensities $I_{in}(\omega_{VIS})$ and $I_{in}(\omega_{IR})$ by an effective surface second-order susceptibility:

$$I(\omega_{SF}) \propto |\chi^{(2)}_{eff}|^2 I_{in}(\omega_{VIS}) I_{in}(\omega_{IR}) \quad (2)$$

The local and nonlocal contributions can be incorporated into $\chi^{(2)}_{eff}$ as elaborated by Shen et al.[20,21,39,40,42] Here we will apply their results for the thin film model outlined above.

We assume that the thin layer is isotropic in the $x-y$ plane, but its properties may change as a function of depth z across the film. Accordingly, we will not consider explicitly the x or y dependence of the fields or material parameters. Under this assumption the incoming electric field is related to that present in the film by the z-dependent Fresnel factors $\vec{\vec{L}}(\omega,z)$ and the local field correction factors $\vec{\vec{l}}(\omega,z)$:

$$\mathbf{E}(\omega,\mathbf{r}) \equiv \mathbf{E}(\omega,z) = \vec{\vec{L}}(\omega,z)\vec{\vec{l}}(\omega,z):\mathbf{E}_{in}(\omega)e^{i(k_x x-\omega t)} \quad (3)$$

where $\vec{\vec{L}}(\omega,z)$ and $\vec{\vec{l}}(\omega,z)$ are diagonal tensors. A similar relationship connects the sum frequency field generated inside the film to that radiated into the substrate. Here, we should emphasize that the calculation of the Fresnel factors $\vec{\vec{L}}(\omega,z)$ for a thin film is different from the well-known infinitesimally thin interface layer model. The effect of multiple reflections inside the thin layer and possible phase variations inside the film should also be considered. Detailed results can be found in the literature.[41,50]

We assume that the thickness d of a thin protein layer is small compared to the wavelengths of the exciting and sum frequency radiation, and the coherence length of the sum frequency generation process. According to the boundary condition, $L_{xx}(\omega,z)$ and $L_{yy}(\omega,z)$ will be continuous across an interface, while $L_{zz}(\omega,z)$ will vary according to the local refractive index.[41,43] If the film is thin enough and the phase variation across the film

is not significant, the Fresnel factors can be written as the following expressions to simplify the discussion:[41,43]

$$L_{xx}(\omega,z) = L_{xx}(\omega)\ ,\ L_{yy}(\omega,z) = L_{yy}(\omega),$$
$$L_{zz}(\omega,z) = L_{zz}(\omega)\frac{n_2(\omega)^2}{n(\omega,z)^2} \quad (4)$$

where $n(\omega,z)$ is the depth-dependent refractive index in the thin layer.

For the thin film model, in addition to the Fresnel factors, we also need to take into account the local field correction factors. By introducing the function

$$f_i(\omega,z) = \left(\frac{n_2(\omega)^2}{n(\omega,z)^2}\right)^{\delta_{iz}} \cdot l_{ii}(\omega,z) \quad (5)$$

where δ_{iz} is the Kronecker delta symbol, substituting (4) into (3), (3) into (1) and (2), considering the Fresnel and local field factors for the sum frequency radiation, and performing a partial integration, we have the final expression for the effective surface second-order susceptibility tensor elements in the thin film model:

$$\chi^{(2)}_{\mathrm{eff},ijk} = L_{ii}(\omega_{\mathrm{SF}})\mathrm{e}_i(\omega_{\mathrm{SF}})\cdot L_{jj}(\omega_{\mathrm{VIS}})e_j(\omega_{\mathrm{VIS}})\cdot L_{kk}(\omega_{\mathrm{IR}})e_k(\omega_{\mathrm{IR}}) \times \chi'^{(2)}_{\mathrm{eff},ijk} \quad (6a)$$

$$\begin{aligned}\chi'^{(2)}_{\mathrm{eff},ijk} = &\int_0^d f_i(\omega_{\mathrm{SF}},z)\chi^D_{ijk}(z)f_j(\omega_{\mathrm{VIS}},z)f_k(\omega_{\mathrm{IR}},z)\,\mathrm{d}z + \\ &\int_0^d f_i(\omega_{\mathrm{SF}},z)\chi^{P_1}_{ijkz}(z)\left[\frac{\partial}{\partial z}f_j(\omega_{\mathrm{VIS}},z)\right]f_k(\omega_{\mathrm{IR}},z)\,\mathrm{d}z + \\ &\int_0^d f_i(\omega_{\mathrm{SF}},z)\chi^{P_2}_{ijkz}(z)f_j(\omega_{\mathrm{VIS}},z)\left[\frac{\partial}{\partial z}f_k(\omega_{\mathrm{IR}},z)\right]\mathrm{d}z + \\ &\int_0^d \left[\frac{\partial}{\partial z}f_i(\omega_{\mathrm{SF}},z)\right]\chi^Q_{ijkz}(z)f_j(\omega_{\mathrm{VIS}},z)f_k(\omega_{\mathrm{IR}},z)\,\mathrm{d}z + \ldots \quad (6b)\end{aligned}$$

where $e_m(\omega_n)$ is the mth component of the polarization unit vector of the nth electric field in medium 2. Note that $\chi'^{(2)}_{\mathrm{eff},ijk}$ contains the z-dependent part of the Fresnel coefficient through the functions $f_i(\omega,z)$. The z-independent parts of the Fresnel coefficients are shown as prefactors.

We note that this formula can be regarded as the application of the general formula obtained by Shen in ref 21 to our experimental situation, with explicit consideration of the local field corrections.

The first integral relates to the dipolar (local) contribution and will be discussed in detail later in sections 2.2 and 3.2, while the others describe the leading order nonlocal contributions, which can be suppressed if the dielectric functions of the ambient and the substrate are matched.[42]

To evaluate the contributions in eq 6, it is necessary to estimate the magnitude of the relevant susceptibility tensors. As in the case of the dipolar susceptibility, higher order susceptibilities are connected to the corresponding molecular hyperpolarizability tensors by a distribution function $G(\theta,z)$ describing both the depth and orientation distribution of the moieties under study with the following definition:

$$N(z) = N_0\int_0^\pi G(\theta,z)\sin(\theta)\,\mathrm{d}\theta \quad (7a)$$

$$N_A \equiv N_0 d = \int_0^d N(z)\,\mathrm{d}z = N_0\int_0^d\int_0^\pi G(\theta,z)\sin(\theta)\,\mathrm{d}\theta\,\mathrm{d}z \quad (7b)$$

where N_0 is the average density (groups/unit volume) of the functional groups under study, thus $N(z)$ is the depth-dependent density profile, N_A is the projected surface density (groups/unit area) and θ is the angle between the molecular ζ-axis and the surface normal (z-direction). This definition gives the following normalization condition for $G(\theta,z)$:

$$\frac{1}{d}\int_0^d\int_0^\pi G(\theta,z)\sin(\theta)\,\mathrm{d}\theta\,\mathrm{d}z = 1 \quad (7c)$$

In this paper, we use the methyl group as an example to deduce the orientation distribution. With the above distribution function, the depth-dependent susceptibility tensors are

$$\chi^D_{ijk}(z) = N_0\int_0^\pi G(\theta,z)\bar{\beta}_{ijk}(\theta)\sin(\theta)\,\mathrm{d}\theta \quad (8a)$$

$$\chi^{P_1}_{ijkl}(z) = N_0\int_0^\pi G(\theta,z)\bar{\beta}^{P_1}_{ijkl}(\theta)\sin(\theta)\,\mathrm{d}\theta \quad (8b)$$

where $\bar{\beta}_{ijk}(\theta)$ and $\bar{\beta}^{P_1}_{ijkl}(\theta)$ (in the lab frame) are orientational averages of the molecular hyperpolarizabilities $\beta_{\alpha\beta\gamma}$ and $\beta^{P_1}_{\alpha\beta\gamma\delta}$ (measured in the molecular frame) over the Euler angles ψ and φ, for which we assume uniform distribution. We have analogous formulas for the other nonlocal susceptibilities. Here, we want to emphasize that Greek indices are in the molecular frame, and Roman indices are in the lab frame.[31]

Although the molecular hyperpolarizabilities can be calculated by molecular modeling software, very little information is published about them in the literature. Therefore, we have to follow a more approximate way. Detailed calculations based on sum-over-states expressions for the molecular response functions show that the resonant molecular hyperpolarizabilities are related to molecular polarizability functions:[51]

$$\beta_{\alpha\beta\gamma} = \frac{B^{D,s}_{\alpha\beta\gamma}}{\omega-\omega_s+i\Gamma_s} \approx -\frac{1}{2\epsilon_0\omega_s}\frac{\partial\alpha_{\alpha\beta}}{\partial q_s}\frac{\partial\mu_\gamma}{\partial q_s}\frac{1}{\omega-\omega_s+i\Gamma_s}$$

$$\beta^{P_1}_{\alpha\beta\gamma\delta} = \frac{B^{P_1,s}_{\alpha\beta\gamma\delta}}{\omega-\omega_s+i\Gamma_s} \approx -\frac{1}{2\epsilon_0\omega_s}\frac{\partial A_{\alpha\beta\gamma}}{\partial q_s}\frac{\partial\mu_\delta}{\partial q_s}\frac{1}{\omega-\omega_s+i\Gamma_s} \quad (9)$$

$$\beta^{P_2}_{\alpha\beta\gamma\delta} = \frac{B^{P_2,s}_{\alpha\beta\gamma\delta}}{\omega-\omega_s+i\Gamma_s} \approx -\frac{1}{2\epsilon_0\omega_s}\frac{\partial\alpha_{\alpha\beta}}{\partial q_s}\frac{\partial Q_{\gamma\delta}}{\partial q_s}\frac{1}{\omega-\omega_s+i\Gamma_s}$$

$$\beta^Q_{\alpha\beta\gamma\delta} = \beta^{P_1}_{\beta\alpha\gamma\delta}$$

where μ, $\overleftrightarrow{\alpha}$, $\overleftrightarrow{A}$, $\overleftrightarrow{Q}$ are the dipole moment, polarizability, electric-dipole−quadrupole polarizability, and quadrupole moment, respectively. The derivatives are taken with respect to the sth normal coordinate, while ω_s and Γ_s denote the frequency and width of the sth normal vibration. Although information on these functions is still very scarce, it seems to be more accessible in the literature than the hyperpolarizabilities themselves. The polarizability function data used for estimation of the hyperpolarizabilities are given as Supporting Information.

Now we can evaluate—at least in an approximate manner—the nonlocal contributions for the polarization combinations relevant in SFG studies. The assumed in-plane isotropy of the film still ensures that only the ssp, sps, pss, and ppp polarization combinations lead to nonzero signals, similar to the case of sum frequency generation from an infinitesimally thin adsorbed layer. For example, in the case of the sps polarization combination only the effective surface susceptibility component $\chi'^{(2)}_{\mathrm{eff},yzy}$ differs from zero. Using eq 6b with the parameters detailed in

the Supporting Material, we have for the nonlocal contribution at the maximum of the resonant peak $\chi'^{P_1}_{\mathrm{eff},yzy} = 0.018 \times 10^{-21}$ m^2/V, $\chi'^{Q}_{\mathrm{eff},yzy} = -0.015 \times 10^{-21}$ m^2/V, and $\chi'^{P_2}_{\mathrm{eff},yzy}$ is expected to be in the same order of magnitude. In the pss polarization combination, $\chi'^{P_1}_{\mathrm{eff},zyy} = -0.015 \times 10^{-21}$ m^2/V, $\chi'^{Q}_{\mathrm{eff},zyy} = 0.018 \times 10^{-21}$ m^2/V, while $\chi'^{P_2}_{\mathrm{eff},zyy}$ is similar.

In the case of the ssp polarization combination $\chi'^{P_1}_{\mathrm{eff},yyz} = \chi'^{Q}_{\mathrm{eff},yyz} = -0.015 \times 10^{-21}$ m^2/V, and $\chi'^{P_2}_{\mathrm{eff},yyz}$ is still expected to be in the same order of magnitude. As far as the ppp polarization combination is concerned, $\chi'^{P_1}_{\mathrm{eff},zzz} = \chi'^{Q}_{\mathrm{eff},zzz} \approx \chi'^{P_2}_{\mathrm{eff},zzz} \approx 0.1 \times 10^{-21}$ m^2/V, while the *xxz*, *xzx*, and *zxx* tensor components are equal to their *yyz*, *yzy*, and *zyy* counterparts.

If we assume that the optical fields change abruptly inside the film, our calculation predicts that the nonlocal contributions increase only 2−3 times in all polarization combinations. If we replace the air ambient with water ($n_1 = 1.34$) and assume that there is no change in the thin film structure, we find that the nonlocal contributions decrease ∼5 times in the *yyz*, *yzy*, *zyy*, *xxz*, *xzx*, and *zxx* tensor components, and ∼8 times in the *zzz* tensor component, as expected. Evaluation of the nonlocal contributions for slightly more ordered distributions reveals no change in their values, which indicates that they are relatively insensitive to small changes in the film structure. We note that Shen et al. deduced values in the same order of magnitude for the nonlocal contributions in the reflected SFG spectra of polyethylene and methanol.[20,24] This result supports our choice for the nonlocal hyperpolarizability. For comparison, our experiments yield a value of $\chi'^{D}_{\mathrm{eff},yyz} \sim 7 \times 10^{-21}$ m^2/V for the symmetric methyl stretch in the ssp polarization combination for a monolayer of BSA at the solution/air interface.[14,16]

According to the above results, if the signal due to a particular molecular vibration is strong (e.g., with an intensity comparable to that of BSA at the solution/air interface), the relative importance of the nonlocal contribution is likely to be very small. In such a case neglect of the nonlocal contributions is appropriate. If the refractive indices of the ambient, the protein layer and the substrate are similar (as in the water ambient), nonlocal contributions induce even less error, at least if the protein signals are strong enough. If, however, the protein signals are too weak, neglect of nonlocal contributions may not be justified.

Our calculations show that the nonlocal contributions are the strongest in the case of the *zzz* susceptibility tensor element, which contributes to the ppp polarization combination. In addition, the local contribution also depends sensitively on the local optical fields, which will be shown in section 3.2. Therefore, evaluation of the ppp-polarized spectrum always requires special attention.

It can be seen from eq 9 that while the local susceptibilities can be resonant only with simultaneously Raman- and IR-active vibrations, the nonlocal contributions can contain other kinds of vibrations (e.g., Raman-active but IR-inactive) as well. As a result, the presence and strength of the latter types of vibrations can serve as an experimental check to judge the relative importance of the nonlocal contributions to the measured spectra as demonstrated in ref 20.

2.2. Local Field Effect on the Dipole Contribution and Determination of Orientation of Functional Groups in Proteins. We showed above that nondipole contributions can usually be ignored. Now we consider only the dipole contribution of the SFG signals collected from the absorbed protein layer. In this case, the effective second-order nonlinear susceptibility $\chi^{(2)}_{\mathrm{eff}}$ of the protein film can be calculated by integrating the depth-dependent dipolar susceptibility weighted by the depth-dependent Fresnel factors and local field correction factors over the whole film. If the film is azimuthally isotropic and thin enough to neglect phase variations, then for different polarization combinations, for example, ssp and sps spectra measured from the reflection direction we have

$$\begin{aligned} x^{(2)}_{\mathrm{eff,ssp}} &= \int_0^d L_{yy}(\omega_{\mathrm{SF}})L_{yy}(\omega_{\mathrm{VIS}})L_{zz}(\omega_{\mathrm{IR}}) \\ &\qquad \sin(\beta_{\mathrm{IR}})f_y(\omega_{\mathrm{SF}},z)f_y(\omega_{\mathrm{VIS}},z)f_z(\omega_{\mathrm{IR}},z)\chi^D_{yyz}(z)\,\mathrm{d}z \\ &= \int_0^d L_{yyz}F_{yyz}(z)\chi^D_{yyz}(z)\,\mathrm{d}z = L_{yyz}\int_0^d F_{yyz}(z)\chi^D_{yyz}(z)\,\mathrm{d}z \\ x^{(2)}_{\mathrm{eff,sps}} &= \int_0^d L_{yy}(\omega_{\mathrm{SF}})L_{zz}(\omega_{\mathrm{VIS}})L_{yy}(\omega_{\mathrm{IR}}) \\ &\qquad \sin(\beta_{\mathrm{VIS}})f_y(\omega_{\mathrm{SF}},z)f_z(\omega_{\mathrm{VIS}},z)f_y(\omega_{\mathrm{IR}},z)\chi^D_{yzy}(z)\,\mathrm{d}z \\ &= \int_0^d L_{yzy}F_{yzy}(z)\chi^D_{yzy}(z)\,\mathrm{d}z = L_{yzy}\int_0^d F_{yzy}(z)\chi^D_{yzy}(z)\,\mathrm{d}z \end{aligned} \tag{10}$$

Both L_{yyz} and L_{yzy} are constants here. In the above equations we introduced the local field weighting factor $F_{ijk}(z)$ to simplify the discussion. $F_{ijk}(z)$ reflects the variation of local optical fields, while β_{VIS} and β_{IR} are the incident angles of the two input beams. Here we will elaborate about the effect of variations in the optical field on dipole contributions. The accuracy of SFG measurements can be affected when this variation is significant. In the infinitesimally thin interface layer model $F_{ijk}(z)$ is treated as a constant across the interface layer, which is valid for most sharp interfaces or small molecule adsorption. For uniform bulk materials, $F_{ijk}(z)$ slowly changes with the optical phase variation along the z direction. However, an adsorbed protein layer with a thickness of several nanometers is thin enough to ignore the phase variation but is too "thick" compared to the range in which the local field correction factor can vary substantially (several angstroms).[46] Since the structure of the protein film is unknown, we cannot simply assume a uniform structure or a constant local optical field across the protein film; we have to evaluate the variation of the local optical field across the thin protein film.

Typically, the local field correction factor usually increases with the increase of the local refractive index. If we evaluate the local field correction factor by the Lorentz model and the protein film is thin enough to ignore the phase variation effect, we find that the values of $F_{ijz}(z)$, $F_{izk}(z)$ and $F_{zjk}(z)$ (here,$i,j,k = x,y$) are not sensitive to a change of local refractive index, and $F_{zzz}(z)$ does change rapidly. For example, if $n(z)$ changes from 1.34 (close to a protein solution) to 1.45 (close to a polymer), $F_{yyz}(z)$ only changes ∼6%, while $F_{zzz}(z)$ changes ∼30%. If $n(z)$ changes from 1.0 (air) to 1.45, $F_{yyz}(z)$ changes ∼20%, and $F_{zzz}(z)$ changes ∼80%. We should point out that any sharp change of a local refractive index of an adsorbed protein film would only happen at boundaries (for example at the protein film/air interface). The Lorentz model is suitable for amorphous bulk material, and here we use it as an approximation for interfaces. If we use the slab model to treat the adsorbed protein/air side of the protein film,[19] the maximum variance of $F_{yyz}(z)$ across the film decreases to ∼5%. Since the picture of the local optical field across a boundary is still not very clear, different models may generate different results. In the following Experimental Section, we will use experiments to test the calculation.

The discussion above shows that for most protein adsorption cases, $F_{yyz}(z)$ or $F_{yzy}(z)$ can be treated as a constant across the protein film. Therefore, SFG spectra collected using ssp and sps polarization combinations can be used to detect the structure of a protein film, while ppp spectra need further analysis. For

ssp and sps spectra, we have

$$x^{(2)}_{\mathrm{eff,ssp}} \approx L_{yyz}F_{yyz}\int_0^d \chi^D_{yyz}(z)\,\mathrm{d}z = L_{yyz}F_{yyz}\chi^{(2)}_{yyz,F}$$

$$x^{(2)}_{\mathrm{eff,sps}} \approx L_{yzy}F_{yzy}\int_0^d \chi^D_{yzy}(z)\,\mathrm{d}z = L_{yzy}F_{yzy}\chi^{(2)}_{yzy,F} \qquad (11)$$

where $\chi^{(2)}_{ijk,F}$ reflects the average orientation and orientation distribution of a chemical group inside the whole adsorbed film, which can be seen if we substitute eq 8a into eq 11. To carry out the *z*-integration in eq 11, we introduced a depth-averaged distribution $\bar{g}(\theta)$:

$$\bar{g}(\theta) = \frac{1}{d}\int_0^d G(\theta,z)\,\mathrm{d}z \qquad (12)$$

and then we have

$$\chi^{(2)}_{ijk,F} = N_0 d\int_0^\pi \bar{g}(\theta)\bar{\beta}_{ijk}(\theta)\sin(\theta)\,\mathrm{d}\theta \equiv N_A\int_0^\pi \bar{g}(\theta)\bar{\beta}_{ijk}(\theta)\sin(\theta)\,\mathrm{d}\theta \qquad (13)$$

i.e., the resulting susceptibility is the angular average of the hyperpolarizability with the depth-averaged distribution.

For adsorbed protein molecules, if we can deduce the average orientation angle and orientation angle distribution of various functional groups, we can achieve a better understanding of their overall structures and conformations. Functional groups such as methyl, methylene, phenyl, and amide can be detected using SFG. The methyl groups are typically end groups of hydrophobic side chains of several amino acids such as valine, leucine, isoleucine, threonine and alanine. These methyl groups can be treated as having C_{3v} symmetry. Aromatic groups are found in amino acids such as phenylalanine, tyrosine and tryptophan. Most amino acids have methylene groups. Both methylene and phenyl groups can be treated as having C_{2v} symmetry. Detailed determinations of average orientation and orientation distributions of several groups including methyl, methylene, and phenyl by SFG have been published.[11−34]

Since the thin film model is applied here, the SFG signal is considered to be contributed from the whole protein layer. To determine orientation information on functional groups, a suitable distribution function must be properly chosen, and such a distribution function must reflect the real orientation distribution. From a mathematical point of view, the best function which can approximate the real distribution is derived from the maximum entropy approach:[30]

$$\bar{g}(\theta) = \exp\left(\sum_{n=0}^{N} a_n \cos^n\theta\right) \qquad (14)$$

We showed in detail how to deduce such a distribution from SFG measurements.[30] However, to simplify the demonstration, in this paper, we will show how to deduce the orientation of methyl groups of BSA at various interfaces using a much simpler model. We believe that it is necessary to emphasize here that to deduce quantitative structural and conformation information about interfacial proteins in the future, the better choice for the orientation distribution function is the function derived from the maximum entropy theory.

3. Experimental Section

3.1. Experimental Arrangement. The experimental setup was similar to that described in our earlier publications and will not be shown.[14,15,30] We used the sample face down geometry, and the input beams traveled through the substrate to overlap at the interface. The incident angles for the infrared and visible beams were 56 and 60°, respectively. In this experiment, the polymer samples were purchased from Scientific Polymer Products Inc. and used as received. The PMMA films were made by spin-coating a 2 wt % solution in toluene on IR grade fused silica substrates (1 in. diameter, $^1/_8$ in. thick, purchased from ESCO products) at 3000 rpm spin speed. Fatty acid free BSA was purchased from Sigma. The protein solution (1 mg/mL) was made by dissolving BSA into deionized water. A right angle IR grade fused silica prism (ESCO products) has also been used to study the silica/protein adsorption with the hypotenuse face contacting the protein solution.

3.2. Evaluation of the Local Field Weighting Factor across the Thin Film for the Dipole Contribution. As mentioned in section 2.2, different models can give different calculated results for the local field weighting factor $F_{ijk}(z)$. Here we want to use experiments to evaluate $F_{ijk}(z)$ across the protein film. From our thin film model, an adsorbed protein layer can be divided into three parts: two interfaces and the layer between them. The local optical field varies with the local refractive index. We assume that the local field weighting factor reaches a maximum value at one interface and a minimum value at the other, and it will vary gradually through the protein layer, from one interface to the other. That is to say, the local field weighting factor inside the film should be intermediate to the two interfaces. If we can prove that the local fields of the two interfaces are similar, then $F_{ijk}(z)$ across the film will not be different. In this case, eqs 11−14 can be used to deduce the orientation and orientation distribution of chemical groups inside the adsorbed protein layer.

If protein molecules are adsorbed at the polymer and protein solution interface, then the adsorbed protein layer can be considered to have two interfaces: the polymer/adsorbed protein interface and the adsorbed protein/protein solution interface. It is difficult to measure the local fields at these two interfaces directly, so we designed an experiment to indirectly deduce the local field weighting factors at these two interfaces. PMMA has a refractive index (1.43) similar to that of the adsorbed BSA layer.[52] When PMMA is in contact with the BSA solution, there is a layer of BSA adsorbed at the polymer surface. The SFG signal of the PMMA surface now actually comes from the buried PMMA/adsorbed protein layer interface. This measurement of the PMMA signal can be used to evaluate the local field weighting factor of the adsorbed protein layer at the polymer/adsorbed protein interface. We then evaluate the local field weighting factor of the PMMA/water interface, which is similar to the interface between the adsorbed protein layer and the protein solution. As mentioned, PMMA has a refractive index similar to that of the adsorbed BSA layer, while the protein solution, which is usually very dilute, has a refractive index similar to that of water. Comparing the local field weighting factor difference between the PMMA/protein solution and PMMA/water interfaces, we can indirectly deduce information about the local fields of an adsorbed protein layer at both interfaces: the PMMA/adsorbed protein interface and the adsorbed protein/protein solution interface.

In addition to the similar refractive indices between PMMA and the adsorbed BSA protein layer, another important reason to choose PMMA to evaluate the local field effect is the fact that the PMMA surface structure does not change appreciably at some interfaces that we investigated, such as the PMMA/air, PMMA/water, and PMMA/BSA solution interfaces. We showed that the PMMA surface is similar in air and water, dominated

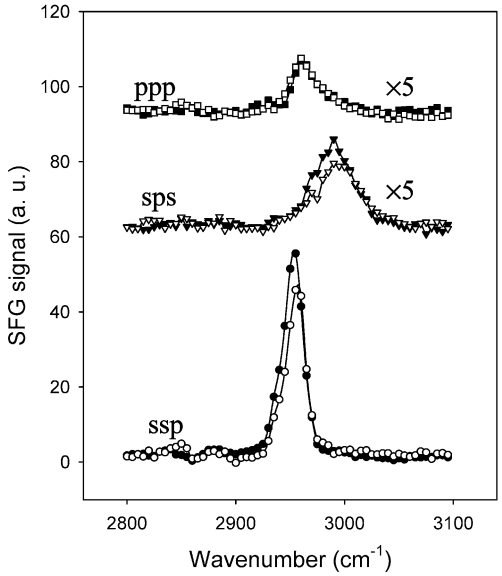

Figure 1. SFG spectra collected from the PMMA/BSA solution interface (filled symbols) and PMMA/water interface (open symbols) using different polarization combinations including ssp, sps, and ppp.

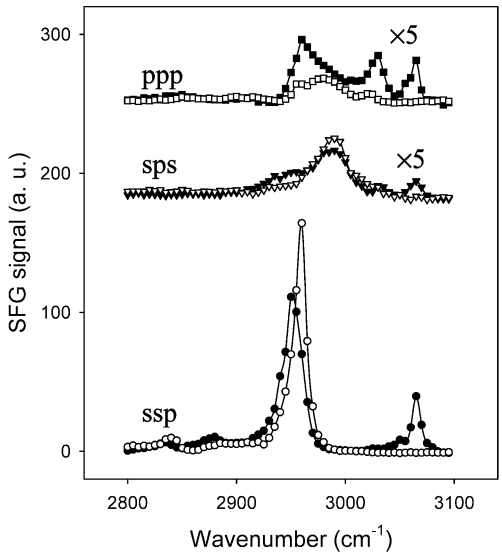

Figure 2. SFG spectra collected from the PMMA/air interface (open symbols) and PMMA covered by a thin layer of PS in air (filled symbols) using different polarization combinations including ssp, sps, and ppp.

in both cases by ester methyl groups.[31,52] In the following we can also prove that it has a similar structure at the PMMA/protein solution interface.

The SFG spectra of PMMA in contact with water and with BSA solution are shown in Figure 1. Our previous SFG spectra of the d-PMMA/BSA solution interface show that a layer of protein will be absorbed at the PMMA/protein solution interface.[15] Even at very low bulk concentrations of the BSA solution, the PMMA surface can be totally covered by adsorbed BSA molecules. Because the adsorbed BSA SFG signal at the d-PMMA/BSA solution interface is very weak, it is ignored here. The SFG spectral features collected from the two interfaces using different polarization combinations are quite similar and are both dominated by the PMMA surface signal, showing that PMMA has similar structures at these two interfaces (Figure 1). Additionally, the SFG signal intensity of the PMMA/water interface is very similar to that of the PMMA/BSA solution interface. This shows clearly that the two interfaces have similar local optical fields. Some small differences in spectral intensity in Figure 1 can be attributed to interference effects of the weak protein signal. This experiment indicates that the local field weighting factors at the PMMA/adsorbed BSA layer and PMMA/water interfaces are quite similar, from which we can deduce that the local fields at the PMMA (or other polymer)/adsorbed BSA protein interface and the adsorbed BSA protein/protein solution interface are quite similar. This result demonstrates that the local field weighting factor variation across the protein layer at the polymer/protein solution interface can be ignored. It agrees very well with our calculated results mentioned in section 2.2. Thus, we can interpret SFG spectra from adsorbed proteins solely by their molecular structure.

Now we will discuss the local field weighting factor for proteins adsorbed at an interface between contacting media with very different refractive indices, e.g., BSA at the polymer/air interface. In this experiment, we also use PMMA as a model. We can consider the local field at the PMMA/PS interface, with a very thin PS layer, to model the local field at the polymer/adsorbed protein interface when adsorbed proteins are exposed to air. We use PS to replace protein such as BSA in this case because BSA molecules generate relatively strong SFG signals in air which will interfere with PMMA. Because the protein layer at the polymer/air interface is very thin, we use a thin layer of PS to more accurately represent the protein film at the PMMA/air interface. We can also consider the PMMA/air interface to evaluate the local field of the adsorbed protein/air interface. The SFG spectra collected from the PMMA/air and the PMMA/PS interfaces are displayed in Figure 2. The buried PMMA/PS interface was made by spin-coating a ~0.1 wt % polystyrene cyclohexane solution on a PMMA surface at 3000 rpm and drying in an oven at 30 °C. The PS film thickness was estimated to be ~10 nm. From the SFG signal intensity of the phenyl group in PS we know that the PMMA surface was completely covered by the PS film. The slight frequency shift of the symmetric C−H stretching mode of the ester methyl groups of PMMA also proves that such an SFG signal comes from the buried PMMA/PS interface.[53] Figure 2 shows that the ssp and sps SFG spectral intensities and features of PMMA at the PMMA/air and buried PMMA/PS interfaces are similar. However, the ppp spectra are different. Our experiments indicate that for these two interfaces, the local field weighting factors for ssp and sps spectra are similar, but those for the ppp spectra are different, which matches our calculations. Our calculations show that the differences of the ppp spectra for these two interfaces are governed by the refractive index changes of the contacting media, not by PMMA interfacial structure changes. The local field weighting factors of the ssp and sps spectra for the PMMA/air and PMMA/PS interfaces are not very different, showing that the local field weighting factor across an adsorbed protein layer on a polymer substrate in air does not vary much. However, it should be pointed out that the ssp and sps SFG signal intensities of the buried PMMA/PS interface are weaker than those in the PMMA/air interface, differing slightly from the calculated result. If we evaluate the local field correction factor by the Lorentz model, the local field weighting factor of the buried interface is larger than the free surface. This difference between the experimental and calculated results is found because either the PMMA surface changes slightly at the buried interface or the local field correction factor calculated by the Lorentz model is too large for this interface. The Lorentz model is valid for amorphous bulk materials; however, an ordered structure like the PMMA surface may cause uncertainties. Another possible reason is that the PS film is not thin enough to

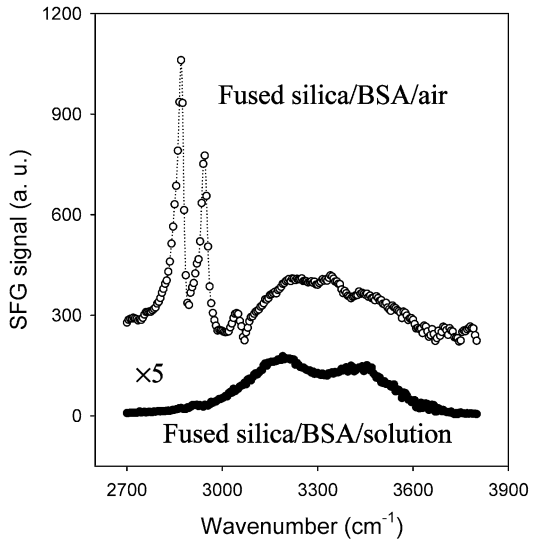

Figure 3. SFG (ssp) spectra collected from the fused silica/BSA solution interface and adsorbed BSA on fused silica exposed to air.

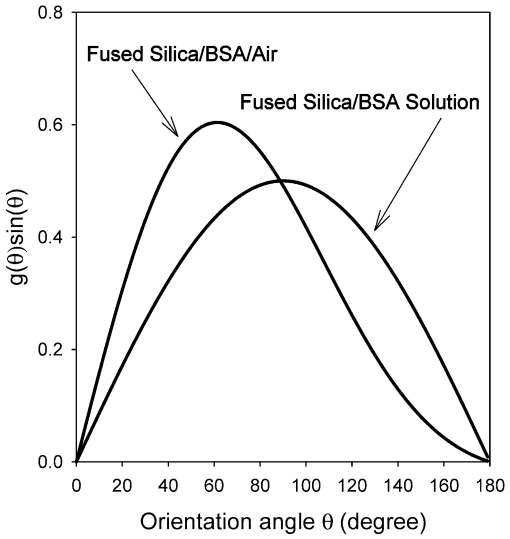

Figure 4. Orientation distributions of methyl groups of adsorbed BSA molecules at the fused silica/BSA solution interface and the fused silica/air interface.

completely ignore the phase effect. Despite these uncertainties, we still found that the local field weighting factor did not change significantly in ssp or sps spectra.

From the experiment and our calculations, we can draw the conclusion that the local field weighting factor $F_{ijk}(z)$ does not vary much across an adsorbed protein layer for ssp and sps polarization combinations for most in situ conditions. As we showed, the calculated nonlocal contributions to the SFG spectra from a protein layer are usually much smaller than the dipole contribution. Therefore, the molecular structures of adsorbed protein molecules can be interpreted by the thin film model addressed above.

3.3. Example: Analyzing Methyl Orientation of BSA at the Fused Silica/Air and Fused Silica/BSA Solution Interfaces. Now we will deduce some very basic quantitative information about adsorbed protein molecules. The SFG spectra of the adsorbed BSA layer at the fused silica/BSA solution and fused silica/air interfaces collected using the ssp polarization combination are used as examples here. The peak assignments were published earlier and will not be repeated.[14−16] To simplify the calculation, a Gaussian distribution function with $\theta_0 = 0$ was chosen here as an approximation. This approach is based on the assumption that the distributions of chemical groups of adsorbed proteins are quite broad; therefore, the distributions are not very sensitive to θ_0. More accurate distributions can be achieved by deducing the values of both θ_0 and σ in the Gaussian function.[30]

The BSA/fused silica interface has already been studied by different techniques, and the surface coverage of BSA on the fused silica surface is known.[54−58] According to neutron reflection measurements, an adsorbed BSA film is close to a monolayer.[55] Here we use a surface coverage of 2.0×10^{12} molecules/cm^2, which is close to our experimental conditions. The absolute SFG intensity of the BSA film on fused silica was measured by comparing the signal to that of *z*-cut quartz.[20,22,30] SFG spectra collected from the adsorbed BSA on fused silica exposed to air and to BSA solution are shown in Figure 3. The orientation distribution functions of methyl groups on the fused silica surface in solution and in air were deduced by the thin film model and are displayed in Figure 4. Detailed methods of spectral fitting and orientation distribution deduction have been published.[14,30] Assuming $\theta_0 = 0$ and using the absolute intensity of the methyl signal, we can deduce the orientation distribution of the methyl groups. From Figure 4, we know that the methyl groups of an adsorbed BSA layer have a symmetric distribution in solution. The symmetric distribution is changed after the adsorbed protein layer is exposed to air, and some methyl groups exhibit preferential alignment. Although this conclusion is very crude, it suggests a possibility of deducing more detailed orientation information about functional groups in adsorbed proteins. By combining the protein selective isotopic label technique,[59] similar studies can provide more conformation information about interfacial protein molecules.

The SFG experiment of BSA at the fused silica/solution interface also confirmed our calculations of nonlocal contributions. According to the theoretical analysis in section 2, the nonlocal contribution is not sensitive to changes of chemical group orientation distribution in the protein layer. Since no C−H signal has been detected for BSA at the fused silica/solution interface, the maximum nonlocal contribution of BSA at this interface must be smaller than the detection limit of our SFG system in the "face down" experimental geometry. We also applied a near total reflection geometry using a prism to improve our detection limit. Even with this experimental geometry, no distinguishable C−H signal has been detected in the SFG spectra, including the ppp spectrum. The absence of C−H signals in the ppp SFG spectrum shows that the nonlocal contributions to its *zzz* susceptibility tensor elements are smaller than the detection limit for the near total reflection geometry ($\sim 0.1 \times 10^{-21}$ m^2/V). This result is compatible with our calculated results for BSA at the fused silica/BSA solution interface. From the calculation, the nonlocal contributions should be smaller than the detection limit of this geometry.

4. Conclusion

In this paper, the thin film model for protein adsorption has been studied both theoretically and experimentally. We want to emphasize that our treatment is significantly different from the infinitesimally thin film model and the general treatment of the "bulk contribution". We have shown that the electric-dipole approximation is in most cases still valid for SFG studies on protein adsorption, and the nondipole contributions can usually be ignored. The experimental results indicate that local field variations across the protein film will not substantially affect

ssp and sps SFG signals. SFG signals collected from adsorbed protein molecules can be used to deduce more quantitative structural or conformation information about such proteins. We also showed that methyl groups of BSA molecules at different interfaces have different orientation distributions.

Acknowledgment. This work is supported by the start-up fund from the University of Michigan, the Office of Naval Research (Grant No. N00014-02-1-0832), Beckman Foundation, National Science Foundation (NATO postdoctoral fellowship for Dr. Zoltan Paszti, Grant No. DGE−0209532, and CHE-0315857), and Dow Corning Corp.

Supporting Information Available: Text giving evaluation of local and nonlocal contributions, further discussions about the local field corrections, and a discussion of the effect of the protein film thickness, including figures showing the density and dielectric function profiles of the adsorbed protein layer used in our calculation on nonlocal contributions, calculated F_{ijk} as a function of local refractive index by using the Lorentz model, model films used to evaluate the slow phase shift effect, and calculated SFG intensities. This material is available free of charge via the Internet at http://pubs.acs.org.

References and Notes

(1) Brash, J. L. Horbett, T. A., Eds. *Proteins at Interfaces, Physicochemical and Biochemical Studies*; American Chemical Society: Washington, DC, 1987.
(2) Baier, R. E. *Applied Chemistry at Protein Interfaces*; American Chemical Society: Washington, DC, 1975.
(3) Horbett, T. A.; Brash, J. L. Eds. *Proteins at Interfaces II, Fundamentals and Applications*; ACS Symposium Series 602; American Chemical Society: Washington, DC, 1995.
(4) Norde, W.; Lyklema, J. *J. Biomater. Sci. Polym. Ed.* **1991**, *2*, 183.
(5) Park, J. B.; Lakes, R. S. *Biomaterials: An Introduction*; Plenum Press: New York, 1992.
(6) Dickinson, E. *Colloids Surf.* **1989**, *42*, 191.
(7) Wynne, K. J.; Guard, H. *Naval Res. Rev.* **1997**, *49*, 2.
(8) Belfer, S.; Fainchtain, R.; Purinson, Y.; Kedom, O. *J. Membr. Sci.* **2000**, *172*, 113.
(9) Ramsden, J. J. *Q. Rev. Biophys.* **1994**, *27*, 41.
(10) Nakanishi, K.; Sakiyama, T.; Imamura, K. *J. Biosci. Bioeng.* **2001**, *91*, 233.
(11) Chen, Z.; Ward, R.; Tian, Y.; Malizia, F.; Gracias, D. H.; Shen, Y. R.; Somorjai, G. A. *J. Biomed. Mater. Res.* **2002**, *62*, 254.
(12) Kim, J.; Cremer, P. S. *ChemPhysChem* **2001**, *2*, 543.
(13) Kim, G.; Gurau, M.; Kim J.; Cremer, P. S. *Langmuir* **2002**, *18*, 2807.
(14) Wang, J.; Buck, S. M.; Chen, Z. *J. Phys. Chem. B* **2002**, *106*, 11666.
(15) Wang, J.; Buck, S. M.; Even, M. A.; Chen, Z. *J. Am. Chem. Soc.* **2002**, *124*, 13302.
(16) Wang, J.; Buck, S. M.; Chen, Z. *Analyst* **2003**, *128*, 773.
(17) Kim, J.; Somorjai, G. A. *J. Am. Chem. Soc.* **2003**, *125*, 3150.
(18) Koffas, T. S.; Kim, J.; Lawrence, C. C.; Somorjai, G. A. *Langmuir* **2003**, *19*, 3563.
(19) Zhuang, X.; Miranda, P. B.; Kim, D.; Shen, Y. R. *Phys. Rev. B* **1999**, *59*, 12633.
(20) Wei, X.; Hong, S. C.; Lvovsky, A. I.; Held, H.; Shen, Y. R. *J. Phys. Chem. B* **2000**, *104*, 3349.
(21) Shen, Y. R. In *Proceedings of the International School of Physics "Enrico Fermi", Course CXX: Frontiers in laser spectroscopy*; Hänsch, T. W., Inguscio, M., Eds. North-Holland: Amsterdam, 1994; p 139.
(22) Oh-e, M.; Lvovsky, A. I.; Wei, X.; Shen, Y. R. *J. Chem. Phys.* **2000**, *113*, 8827.
(23) Wei, X.; Hong, S. C.; Zhuang, X.; Goto, T.; Shen, Y. R. *Phys. Rev. E* **2000**, *62*, 5160.
(24) Superfine, R.; Huang, J. Y.; Shen, Y. R. *Phys. Rev. Lett.* **1991**, *66*, 1066.
(25) Gragson, D. E.; Richmond, G. L. *J. Phys. Chem.* B **1998**, *102*, 3847.
(26) Yang, C. S. C.; Richter, L. J.; Stephenson, J. C.; Briggman, K. A. *Langmuir* **2002**, *18*, 7549.
(27) Briggman, K. A.; Stephenson, J. C.; Wallace, W. E.; Richter, L. J. *J. Phys. Chem. B.* **2001**, *105*, 2785.
(28) Bain, C. D. *J. Chem. Soc., Faraday Trans.* **1995**, *91*, 1281.
(29) Chen, Z.; Shen, Y. R.; Somorjai, G. A. *Annu. Rev. Phys. Chem.* **2002**, *53*, 437.
(30) Wang, J.; Paszti, Z.; Even, M. A.; Chen, Z. *J. Am. Chem. Soc.* **2002**, *124*, 7016.
(31) Wang, J.; Chen, C. Y.; Buck, S. M.; Chen, Z. *J. Phys. Chem. B* **2001**, *105*, 12118.
(32) Chen, C. Y.; Even, M. A.; Wang, J.; Chen, Z. *Macromolecules* **2002**, *35*, 9130.
(33) Gautam, K. S.; Dhinojwala, A. *Phys. Rev. Lett.* **2002**, *88*, 145501.
(34) Henry, M. C.; Yang, Y.; Pizzolatto, R. L.; Messmer, M. C. *Langmuir* **2003**, *19*, 2592.
(35) Opdahl, A.; Somorjai, G. A. *Langmuir* **2002**, *18*, 9409.
(36) Baldelli, S.; Mailhot, G.; Ross, P. N.; Somorjai, G. A. *J. Am. Chem. Soc.* **2001**, *123*, 7697.
(37) Baldelli, S.; Markovic, N.; Ross, P. N.; Shen, Y. R.; Somorjai, G. *J. Phys. Chem. B* **1999**, *103*, 8920.
(38) Heinz, T. F. In *Nonlinear Surface Electromagnetic Phenomena*; Ponath, H.-E., Stegeman, G. I., Eds.; Elsevier: Amsterdam, 1991; p 353.
(39) Guyot-Sionnest, P.; Chen, W.; Shen, Y. R. *Phys. Rev. B* **1986**, *33*, 8254.
(40) Guyot-Sionnest, P.; Shen, Y. R. *Phys. Rev. B* **1988**, *38*, 7985.
(41) Wilk, D.; Johannsmann, D.; Stanners, C.; Shen, Y. R. *Phys. Rev. B* **1995**, *51*, 10057.
(42) Guyot-Sionnest, P.; Shen, Y. R. *Phys. Rev. B* **1987**, *35*, 4420.
(43) Shen, Y. R. *Appl. Phys. B: Laser Opt.* **1999**, *68*, 295.
(44) Held, H.; Lvovsky, A. I.; Wei, X.; Shen, Y. R. *Phys. Rev. B* **2002**, *66*, 205110−1.
(45) Ekhoff, J. A.; Rowlen, K. L. *Anal. Chem.* **2002**, *74*, 5954.
(46) Ye, P.; Shen, Y. R. *Phys. Rev. B* **1983**, *28*, 4288.
(47) Eisert, F.; Dannenberger, O.; Buck. M. *Phys. Rev. B* **1998**, *58*, 10860.
(48) Simpson, G. J. *J. Chem. Phys.* **2002**, *117*, 3398.
(49) Pershan, P. *Phys. Rev.* **1963**, *130*, 919.
(50) Sipe, J. E. *J. Opt. Soc. Am. B* **1987**, *4*, 481.
(51) Cho, M. *J. Chem. Phys.* **2002**, *116*, 1562.
(52) Wang, J.; Woodcock, S. E.; Buck, S. M.; Chen, C. Y.; Chen, Z. *J. Am. Chem. Soc.* **2001**, *123*, 9470.
(53) Liu, Y.; Messmer, M. C. *J. Am. Chem. Soc.* **2002**, *124*, 9714.
(54) Kurvat, R.; Prenosil, J. E.; Ramsden, J. J. *J. Colloid Interface Sci.* **1997**, *185*, 1.
(55) Su, T. J.; Lu, J. R.; Thomas, R. K.; Cui, Z. F.; Penfold, J. *J. Phys. Chem. B* **1998**, *102*, 8100.
(56) Giacomelli, C. E.; Norde, W. *J. Colloid Interface Sci.* **2001**, *233*, 234.
(57) Norde, W.; Giacomelli, C. E. *J. Biotechnol.* **2000**, *79*, 259.
(58) Norde, W.; Anusiem, A. C. I. *Colloids Surf.* **1992**, *66*, 73.
(59) Wang, J.; Clarke, M. L.; Zhang, Y.; Chen, X.; Chen, Z. *Langmuir* **2003**, *19*, 7862.